Macromolecular Materials and Engineering
Open Access
www.mame-journal.de

High Dose Progesterone Loaded PCL-Polysorbate 80 Transdermal Fibers for Potential Application in Gynecological Oncology

*Omar Shafi, Saurabh Phadnis, Un Hou Chan, Mohan Edirisinghe, and Francis Brako**

Progesterone (P4), commonly administered in high doses for endometrial cancer palliative management, has limitations in current delivery systems. This preliminary in vitro drug release study introduces electrospun patches to offer a new perspective on P4 delivery. The study aimed to assess the influence of the surfactant polysorbate 80 (PS80) on the release of P4 from polycaprolactone (PCL) fibers. The PS80 effects are examined to inform the fine-tuning of the fibre generation process. Patches developed, PCL wet (with PS80) and PCL dry (without PS80), showed encapsulation efficiencies of 76% and 42%, respectively. The dose levels studied are 6.1 mg for PCL wet and 4.4 mg for PCL dry samples. Molecular studies show that higher surfactant levels improved P4-polymer mixing, enhancing dissolution and release rates. Patches with PS80 released 66% of the drug in 17 h, while those without released only 51%. Release data best fit the Weibull model, showcasing promise for these patches in transdermal P4 delivery. This study offers a non-invasive option compared to traditional methods and underscores the need for further research to confirm the patches' clinical effectiveness for potential use in gynecological oncology.

1. Introduction

Gynecological cancers represent nearly 20% of all new cancer cases worldwide and about 12% in the UK.[1,2] Endometrial cancer, the most prevalent gynecological cancer in developing countries and the fourth most common in the UK, accounted for ≈250 000 cases and 62 000 deaths globally in 2005, making up 60% of the global burden.[1] This cancer primarily affects the endometrium and constituted around 5% of all new cancer cases between 2016 and 2018.[3,4] Although the total number of endometrial cancer cases is high, around 70% are localized to the uterine cavity at stage 1, with 92% of patients surviving the disease.[4,5] However, if extraperitoneal metastases occur and the cancer spreads to other anatomical locations, such as the para-aortic nodes, the 5-year survival prognosis worsens six times.[4,6] Without optimal cancer services, patients are at risk of preventable disease progression. The outlook was further worsened by COVID-19, exacerbating the NHS backlog.[7] By January 2021, primary care contacts and urgent cancer referrals reduced by 20% (95% CI 18.1–22.3%), for gynecological cancers alone by 10.3% (95% CI 9.7% to 10.9%), and one in four patients failed to meet the 62-day cancer waiting target from initial suspicion to commencement of treatment.[8] The critical impact of early detection on endometrial cancer outcomes emphasizes the urgent need for improved services. Yet, political conflicts of interest impede optimal care delivery.[8] At the early, recognizable stages of endometrial cancer, patients can present with abnormal bleeding which is amongst the "red flags" symptoms of the disease.[5,9] Early assessment and treatment of endometrial cancer are facilitated by hysteroscopic examinations, endometrial thickness investigations, and biopsies. In areas with limited healthcare access, preventable treatments are often neglected, leading to worsening cases and highlighting the concept of the inverse care law. This underscores the critical need for accessible treatment options.[10]

P4 plays a crucial role in palliating endometrial cancer symptoms by countering the proliferative effects of estrogen, inhibiting cell differentiation and growth. It prevents cancerous tissue growth in patients undergoing hormone replacement therapy (HRT) and effectively controls excessive bleeding symptoms.[11,12] For cases considering fertility preservation and stage 1 endometrial cancer, P4 offers an alternative to invasive procedures like hysterectomy and bilateral

O. Shafi, U. H. Chan, M. Edirisinghe
Torrington Place, Department of Mechanical Engineering
University College London (UCL)
London WC1E 6BT, UK
S. Phadnis
London Gynaecology
15 Austin Friars, London EC2N 2HE, UK
F. Brako
Faculty of Engineering and Science, Department of Science
University of Greenwich
Chatham ME4 4TB, UK
E-mail: f.brako@greenwich.ac.uk

The ORCID identification number(s) for the author(s) of this article can be found under https://doi.org/10.1002/mame.202300447

DOI: 10.1002/mame.202300447

salpingo-oophorectomy (removal of sex organs).[13] Additionally, P4 treatment benefits patients with multiple comorbidities for whom surgery is not an option, highlighting the importance of effective delivery.[13] In advanced/recurrent endometrial cancer management, HRT with high-dose P4 is combined with other therapies, including chemotherapy, guided by histopathology and clinical factors.[14] At the European Consensus Conference for Endometrial Cancer, a unanimous 100% consensus supported the use of high-dose P4 for specific clinical scenarios, such as grade 1 or 2 endometroid tumors and/or recurrent disease biopsies.[14]

P4 can be initially given as an intravaginal coil. However, when women decline or do not respond to the coil's 20 µg per day dosage, guidelines suggest a supplementary approach with a higher oral dosage of 200 mg daily.[15] Due to the hepatic bypass effect, oral delivery results in reduced bioavailability (typically ranging from 5% to 15%), necessitating a higher dose to compensate for the percentage wasted. The ultimate goal is to achieve a daily dosage of approx. 20 mg of P4.[14] The current delivery methods described have their limitations. P4 injections carry infection risks under unsanitary conditions, and patients in poorer communities may lack access to proper administration by clinicians. Dysphagia can also cause discomfort with oral P4 medication, and first-pass hepatic metabolism further reduces its oral bioavailability.[16,17] Rectal and intravaginal P4 medication also present barriers to patients due to their intimate, discomforting delivery methods.[18] Although P4 patches for HRT and contraception exist (Evorel Sequi and Evra), they contain estrogen, which may not always be required, and have specific dosages for different conditions.[19,20] Hence, while existing approaches are available, the constraints associated with them could be addressed through the utilization of non-invasive transdermal fibrous patches delivering P4 exclusively. These patches can be tailored to meet specific clinical requirements, presenting a hopeful alternative to current delivery methods that face compliance challenges. This study focuses on producing high-dose fibrous P4-loaded patches for potential future drug delivery to address these patient requirements.

Polymeric fibrous patches are emerging as a promising tool in transdermal drug delivery. Their tunable characteristics, such as porosity, facilitate the diffusion and dissolution of drugs from the fibrous structure.[21,22] Upon release from these fibers at a designated particle size (with molecules having a kDa weight less than 400), the drug encounters the stratum corneum.[23] Through passive diffusion, it then progresses via intercellular pathways within the lipid matrix, advancing to the epidermis, and ultimately accessing the capillaries to enter the bloodstream.[23,24] Surfactants can enhance intralipid transport through several mechanisms, including increasing permeability by modifying lipid structures decreasing lipid resistance of drug, minimizing drug crystallinity, and fostering a more moist environment.[25,26]

A polymeric drug delivery system has been employed due to its strong affinity to active substances.[27,28] Electrospinning (ES) is a successful method used in this study to create P4 patches, demonstrating its potential for fabricating uniform drug delivery systems.[28] Previous studies have demonstrated the promising potential of infusing P4 into fibers using polymers such as zein and polyvinylpyrrolidone. This warrants further exploration of alternative polymer options to expand our understanding in this area.[29,30] The process involves injecting a polymer solution at a constant, chosen rate of liters per unit time through a needle which is attached to a high-voltage ramp. The solution is then electrospun onto a collection plate which is at a chosen height below the needle. Due to the electric field created between the needle and collector plate, the jet stream is altered from a circular shape to a conical Taylor cone, which experiences whipping and bending instabilities as it travels. The jet finally collects on the conductive plate, leaving behind a circular patch of fibers as the solvent evaporates. The fibers that remain contain the chosen additive, and in this case, P4. The patch is then peeled off the plate. Various external factors, such as temperature, humidity, and solution properties, can affect the morphology of the fibers.[29,31]

Polycaprolactone (PCL), a biocompatible and biodegradable polymer, is used in this study due to its rubbery state resulting in high toughness and impressive mechanical properties such as high strength and elasticity.[32,33] The polymer is non-toxic and tissue-compatible and has found a strong presence in scaffolds for regenerative therapy and drug delivery.[34,35] Acetone, an essential solvent for dissolving PCL, exhibits superior solubility for P4 compared to other solvents like ethanol, enabling a high level of drug incorporation. The combination of PCL and acetone opens up possibilities for creating a diverse range of P4 only patches with varying drug doses in smaller volumetric spaces, creating lighter weight P4 patches. Moreover, at the concentrations used in the study, acetone is non-toxic, ensuring the safety of the process. Additionally, acetone conveniently evaporates from the fibers during production, leaving behind P4-loaded patches.[36,37] This allows the drug and polymer to be easily dissolved into one polymer solution prior to adding PS80. For gynecological oncology, it is important to be able to maximize P4 dissolution into solvent to infuse the highest amount of P4 into the potential transdermal patch scaffold.

In this study, PS80, a non-ionic surfactant commonly used in the cosmetic and skin industry, was used to enhance permeation in the patch and achieve a more uniform transdermal structure by reducing bead formation.[25,38-40] Notably, PS80's non-ionic nature contributes to its lower irritation potential compared to cationic and anionic surfactants, thereby reducing the risk of contact dermatitis.[41] This allows a more controlled approach to drug release and as it acts as a surface penetration enhancer, PS80 can potentially improve drug delivery through membranes including skin.[34] This investigation releases drugs into a non-toxic phosphate buffer saline (PBS). PBS is widely used in transdermal research due to its ability to maintain a pH of 7.4, mirroring fluids of the human body.[42-44] The osmolarity and ion concentration closely bear a resemblance to that of blood serum, rendering it a suitable medium for the in vitro study and to create a path for future investigations.[29] This preliminary in vitro drug release study provides a clearer picture for the potential of the patch for further clinical studies.

2. Experimental Section

2.1. Materials

PCL with a molecular weight of ≈80 g mol^{-1}, P4 with a molecular weight of around 314 g mol^{-1} and an aqueous solubility of 8.81 mg L^{-1}, phosphate buffer saline (PBS) with a pH level of 7.4,

Table 1. Addition of Polysorbate to 20 mL of 9% w/v PCL solution.

Sample	PCL ($w_{Polymer}/v_{solvent}$)	Acetone [mL]	P4 ($w_{drug}/v_{Solvent}$)	PS80 ($V_{PS80}/V_{solvent}$)
1	9%	20	12.5%	0%
2	9%	20	12.5%	15%
3	9%	20	12.5%	20%
4	9%	20	12.5%	25%
5	9%	20	12.5%	30%

Table 2. Final Solution Reagents used to generate fibers for drug release. See Table 1, sample 2.

Reagents	PCL Blank	PCL Dry	PCL wet
PCL [g]	1.8	1.8	1.8
Acetone [mL]	20	20	20
P4 [g]	0	2.5	2.5
Polysorbate [mL]	0	0	3

PS80 (1310 g mol^{-1}), and acetone which was used as a solvent in this study were purchased from Sigma-Aldrich, Gillingham, UK. The cellulose acetate membranes with a pore size of 0.2 µm that were used for the permeation studies were purchased from Sartorius, Gottingen, Germany. All the chemicals were used as received without any further purification.

2.2. Solution Preparation and Characterization

Five solutions were initially electrospun, 8%, 9%, 10%, 11%, and 12% (**Table 1**). The solution with the lowest diameter and smallest standard deviation was chosen for the continuation of the study, see Figure S1 (Supporting Information). Therefore, a 9% solution of PCL (1.8 g in 20 mL Acetone) was used in all experiments. As shown in Table 1, 3, 4, 5, and 6 mL volumes of PS80 were added to each of the 9% PCL solutions (respective volumes shown as $v_{PS80}/v_{solvent}$). Each solution was under constant magnetic stirring, at 50 °C, for an hour. PCL polymer solutions with PS80 were named "wet" and without the surfactant, "Dry." PCL solutions with no other reagents or drugs were named as "blank." Uniform mixtures of PCL blank, PCL dry, and PCL wet were used in electrospinning after scanning electron microscope analysis (shown in **Table 2**).

The solutions' viscosities were measured using a calibrated Brookfield Viscometer DV-III+ (Brookfield, Middleboro, MA, USA) calibrated to determine the viscosity at the shear rate required to produce 99% torque for each solution. Additionally, the surface tension for each solution was determined using a Tensionmeter (Kruss GmbH, Hamburg, Germany) that had been calibrated beforehand.

2.3. Preparation and Characterization of Fibers

After complete dissolution, the solution was prepared for electrospinning. Each solution underwent a 5-min spinning process at a constant flow rate of 160 µL min^{-1} and a voltage of ≈10 kV, under ambient temperature conditions of ≈21 °C and humidity of ≈50%. Following the spinning process, all solution products were imaged using a scanning electron microscope. The solution that produced fibers with the smallest diameter was selected for P4 loading. The maximum solubility of P4 in acetone was determined to be 125 mg mL^{-1}. To prepare the fibers for imaging, 2.5 g of the drug was dissolved in 20 mL of acetone, and the corresponding PCL and polysorbate solutions were collected on carbon-taped SEM studs. Subsequently, the fibers were coated with gold for 90 s using a Q150R ES (Quorum Technologies) sputter coater and analyzed through scanning electron microscopy (SEM, the Hitachi S-3400n) at an accelerating voltage of 5 kV. The fiber diameters were measured using ImageJ, and the data was analyzed and presented using Python and OriginPro to create a distribution plot of the various fiber diameters. Approximately 100 random fibers from three patches for each sample were examined. Each sample was remade using a new batch of the same solution ratios. Solvent residue in electrospun fibers (Table 4) were also calculated by measuring the mass of fibers immediately after electrospinning and comparing this to the calculated dry mass of polymer and additives. The initial mass of the solvent, determined from the volume used in the solution, was recorded. The difference in mass between the electrospun fibers and the initial dry components indicated the solvent residue.

2.4. Drug Loading and Release

For this study, drug release characteristics were analyzed spectrophotometrically at 270 nm using a Jenway 6305 UV/visible spectrophotometer (Bibby Scientific, Staffordshire, UK).[45,46] PS80 (from Aldrich) displays a marked absorption at 234 nm, after which its absorption decreases considerably.[47,48] In this study, a fixed 5 mL volume in the Franz diffusion cell was selected to examine the drug's release dynamics from the polymer. This approach ensured the drug consistently tended toward its maximum saturation point, providing insights into drug release in a set space and facilitating a better understanding of polymer-drug interactions. Saturation in this consistent volume allowed for direct comparisons between different formulations, highlighting their distinct performance. Two main parts were conducted, focusing on the calculation of the actual drug content in the patches and the assessment of drug release. A reference blank sample of 5 mg fibers with no drug was measured using a UV machine at 270 nm. A test sample containing 11.9 mg fibers (either PCL dry or PCL wet) with the drug was compared against these 5 mg blank fibers to account for a 138% increase in overall polymer weight due to P4 addition. This was consistent throughout the entire drug release study. For the first part, a calibration curve (P4calicurve) was generated to determine the concentration of P4 in acetone. The calibration curve was used to calculate the exact drug content in the PCL dry and wet fiber patches that were being tested. The encapsulation efficiency was also calculated by dividing the actual amount by the theoretical expectation. In the second part, a comparative absorbance method was employed to record the drug release behavior. Two additional calibration curves (drycalicurve and wetcalicurve) were established to determine the relationship between P4 content and patch weight in phosphate-buffered saline (PBS). From drycalicurve and wetcalicurve, the maximum absorbance values for PCL dry and PCL wet were determined. These samples were fully submerged in PBS

Table 3. Equations used for Predictive Modeling.[51-53]

Model	Equation	Parameters
Baker Lonsdale	$\frac{3}{2}(1-(1-\frac{F}{100})^{\frac{2}{3}})-\frac{F}{100}=k_{BL}\times t$	F is the fraction of release, k_{BL} is the release rate constant, t is time.
Higuchi	$F=k_H\,t^{0.5}$	k_H is the release rate constant, t is time.
Gompertz	$F=100e^{(-\alpha e^{(-\beta\log(t))})}$	The model describes α as the undissolved proportion at time $t=1$, serving as a location or scale parameter, and β as the dissolution rate per unit time, serving as a shape parameter. The model shows a rapid increase at the beginning and a slow convergence toward the maximal dissolution asymptote.
Korsemeyer Peppas	$F=k_{KP}\,t^n$	The release mechanism is characterized by the value of n, which can be determined by the slope of the straight line (where F is the on the y axis and t on the x), while the release rate constant is denoted as k_{KP}. For a cylindrical matrix, the value of n determines the type of release mechanism. For example, a value of $n=0.45$ indicates Fickian release (case I), while a value between 0.45 and 0.85 indicates non-Fickian (anomalous) release. A value of $n=0.89$ indicates case II (zero-order release), and a value greater than 0.89 indicates super case II type release. The variable t represents time.
Makoid Banakar	$F=k_{MB}\,t^n e^{-kt}$	k_{MB} = release rate constant, n and k are empirical factors where $k>0$.
Peppas Sahlin	$F=k_1\,t^m+k_2 t^{(2m)}$	The constant k_1 is related to Fickian kinetics, while the constant related to case-2 relaxation kinetics is denoted as k_2. The diffusional exponent m applies to devices of any geometric shape that impede controlled release.
Probit	$F=100\varphi(\alpha+\beta\log(t))$	In this model, the variable φ represents the standard normal distribution, while α serves as the scale factor, and β represents the shape factor.
Weibull	$F=100(1-e^{-\frac{(t-T_i)^\beta}{\alpha}})$	In the given model, α denotes the time process, Ti represents the time lag, and β serves as the shape parameter. The value of β determines whether the curve is exponential ($\beta=1$), S-shaped with an upward curve followed by a turning point ($\beta>1$), or parabolic with a higher initial slope, indicating the exponential ($\beta<1$).
Hopfenberg	$F=100[1-(1-k_{HB}t)^n]$	k_{HB} is the combined constant, where $k_{HB}=\frac{k_0}{C_0\times a_0}$, the erosion rate constant is represented by k_0, while C_0 denotes the initial drug concentration within the matrix, and a_0 represents the radius of the cylinder. For a cylindrical matrix, the value of n is 2.
Geometric Equation	$Q(t)=\tan h(\frac{\gamma(Dt)^{1/2}}{a})$	The diffusion constant is denoted by D, while a refers to the cylinder's radius, and γ is a constant value.

(receptor volume 5 mL), stirred magnetically for 24 h to achieve maximum internal drug release, and the absorbance at this stage was recorded as the final reference. The drug release was finally conducted, whereby 11.9 mg of P4-loaded patches were placed on top of cellulose acetate membranes, releasing into a Franz diffusion cell (reception volume 5 mL). A reading was taken at time points and after each reading, the samples were returned to the cells for subsequent measurements. Differences in drug release were recorded at various time points until reaching the maximum absorbance determined earlier. The top of the diffusion cell orifice with a 25.4 mm outer diameter was covered with parafilm and pierced to increase pressure in the fiber system. Given the transdermal nature of this study, the cell was maintained at a constant temperature of 35 °C to mimic skin temperature. To ensure proper mixing of P4 transported through one membrane into the buffer solution of the accepting chamber, a magnetic stirrer was employed in the bath. To ensure accuracy, all tests were conducted in triplicate using three separate samples for each set.

2.5. Molecular Characterization of Fibers by Fourier Transform Infrared Spectroscopy

Fourier transform infrared spectroscopy (FTIR) spectroscopy (PerkinElmer Spectrum 100) was employed to analyze the relationships between the drug, polymers, and chemical reaction within the processed fibers. Before analysis, 2 mg of each sample (PCL Blank, PCL dry, and PCL wet) were placed on the ATR crystal and studied over ten times in the range of 500–4000 cm^{-1} at a resolution of 4 cm^{-1}. The experiment was conducted three times, using three distinct samples for each repetition.

2.6. Drug Release Modeling

Ten mathematical models described in **Table 3** compared the experimental drug release to predictive kinetic and geometric models. DDSolver was used for kinetic models and MATLAB was used for the geometric equation.[49,50] (**Table 4**)

2.7. Statistical Analysis

T-tailed *t*-tests were performed to assess the significance of drug release and diameter variations between wet and dry fibers. The corresponding *P*-values can be found in Section 3. The mean of the root mean square errors (RMSE) of both dry and wet fibers quantified the differences between predicted and observed drug release.

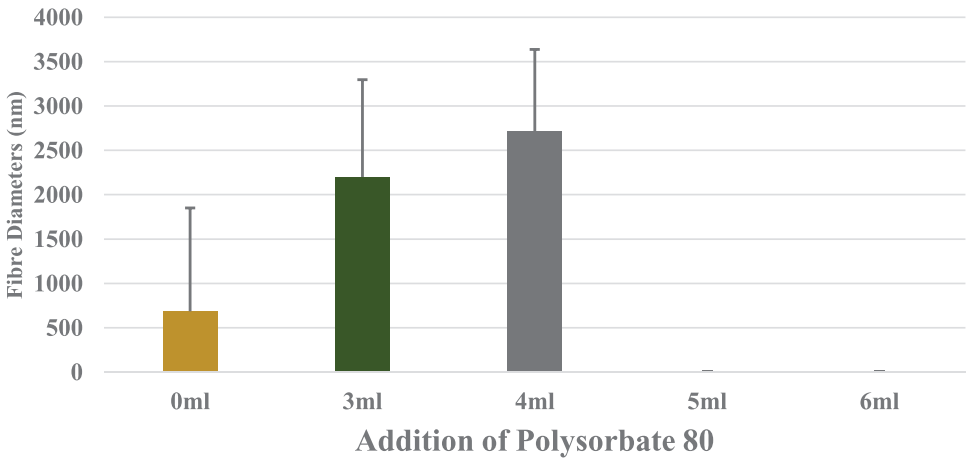

Figure 1. The influence of PS80 on the fiber diameters generated from 9% PCL. Increasing the PS80 amounts in solutions increased the fiber diameters. For each patch, 100 random fibers were analyzed. No viable fibers were formed when adding 5 or 6 mL's to the solution.

Table 4. Physical properties of polymer solutions and solvent residue in resulting fibers.

Property	PCL Blank	PCL Dry	PCL wet
Concentration of Polymer($w_{PCL}/v_{Solvent}$)%	9	9	9
Concentration of PS80($v_{PS80}/v_{Solvent}$)%	0	0	20
Concentration of Drug($w_{P4}/v_{Solvent}$)%	0	12.5	12.5
Temperature [°C]	21	21	21
Viscosity [mPa s]	12.3 ± 1.2	14.9 ± 1.1	12 ± 2.2
Surface Tension [mN m^{-1}]	22.7 ± 0.6	23.4 ± 0.1	20.8 ± 0.1
Solvent Residue in Fibers [%]	0.19 ± 0.13	0.21 ± 0.18	1.12 ± 0.16

3. Results and Discussion

3.1. Solution Properties

The rheometer spindle's torque, when increased to 99%, revealed the changes in viscosity across each solution. When adding P4 to the "blank" solution, the viscosity increased from 12.3 to 14.9 mPa s. When polysorbate was then added, the viscosity reduced to 12 mPa s. A similar phenomenon was observed with surface tension analysis. When adding P4 to PCL Blank, the surface tension increased from 22.7 to 23.4 mN m^{-1}. Upon adding polysorbate, the surface tension reduced to 20.8 mN m^{-1}. The decrease in viscosity and surface tension when introducing PS80 confirms the reduction in interfacial tension within the solution and the shrinking of polymer chains.[54] The addition of P4 and PS80 to the PCL Blank solution for fibers increased solvent retention from 0.19% to 0.21% with the drug, and markedly further to 1.12% with polysorbate 80, reflecting the surfactant's impact on solvent evaporation efficiency. This notable difference can be attributed to the morphological changes seen when adding PS80, see Figure 2.[55]

3.2. Fiber Formation and Morphology

Polysorbate was added to the fixed polymer solution, with increments of 1 mL from 3–6 mL. Without the surfactant, fibers formed were in the nanometer range. However, once surfactant was added, the diameters increased into the micrometer range. PS80 is known to increase the electrical conductivity in polymeric solutions, altering the electric field and charge distribution during spinning, therefore leading to thicker fibers being formed.[56] When more than 4 mL of polysorbate was introduced, the solutions exhibited two outcomes: either the fibers would embed within one another, or no fibers would be observed at all (refer to **Figure 1**). In the viable patches, adding PS80 reduced the standard deviation suggesting an improvement in homogeneity within the patches as seen in Figure 1, decreasing from 1165 to 929 nm. The skeleton chosen was Sample 2, see Table 1. This solution had the lowest fiber diameters with the highest amount of polysorbate to aid transdermal drug permeation. Loading P4 into the fibers did not result in any noticeable diameter difference, as shown in Figure S3 (Supporting Information). Both PCL Blank and PCL dry exhibited a diameter of 700 nm, and there was no statistically significant difference between them ($p > 0.05$). However, the addition of P4 led to an increase in the standard deviation among the fibers, ±480 to ±1170 nm, indicating a reduction in patch homogeneity. Figure 5 shows the effect of PS80 on diameter—the diameter increased by 70% from 700 to 2200 nm. PS80 decreased the appearance of beads formed in the fibers as seen in Figures 2a,b, improving homogeneity across the patch. The diameters from three samples were analyzed for both PCL dry and PCL wet using ImageJ. The average diameter distributions can be seen in **Figure 2**c. The peaks of the curve describe the average diameter as mentioned above.

3.3. Molecular Characterization by Fourier Transform Infrared Spectroscopy

For PCL in **Figure 3**B–D, characteristic peaks are displayed at 2930 and 2866 $cm^{-1,}$ exhibiting CH_2 asymmetric and symmetric stretching, respectively.[57] There are also peaks at 1730 cm^{-1} (carbonyl stretching), 1294 cm^{-1} (C—O and C—C stretching in crystalline phase), 1240 cm^{-1} (asymmetric C—O—C stretching), 1190 cm^{-1} (O—C—O stretching), 1170 cm^{-1} (symmetric

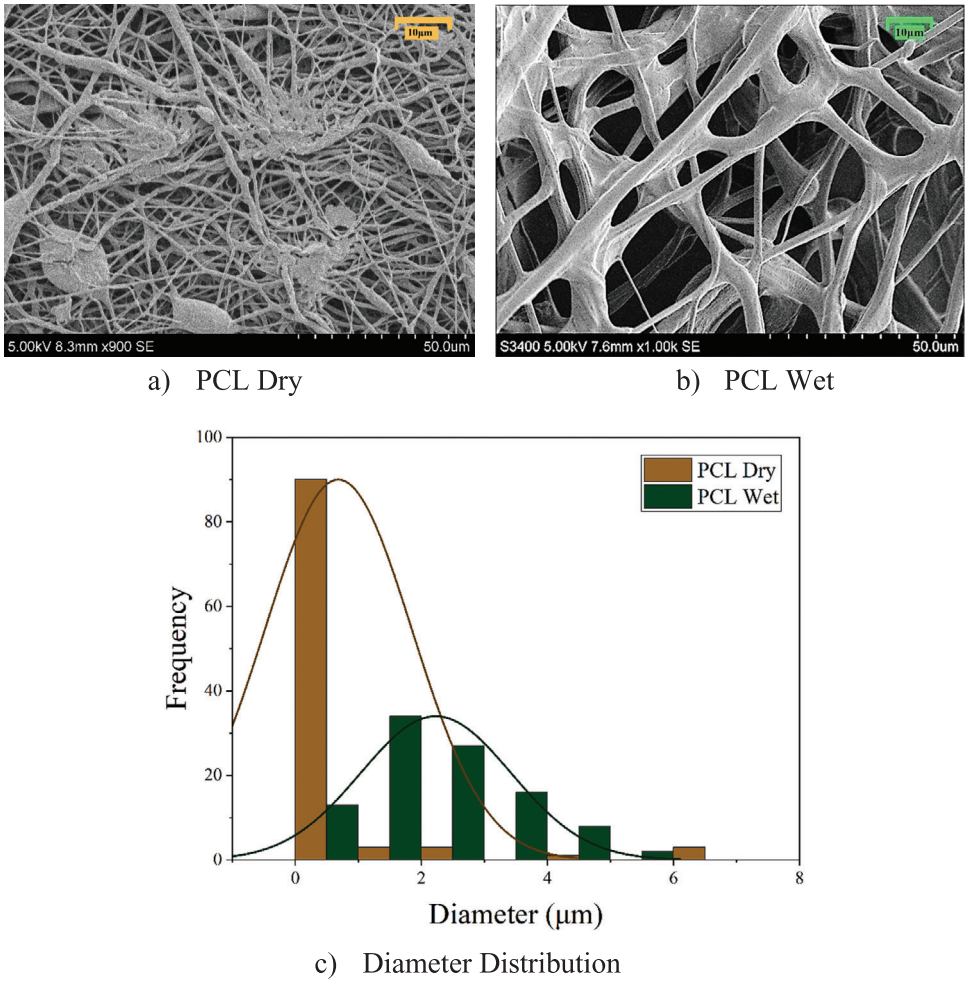

Figure 2. SEM images of a) dry fibers, and b) wet fibers, and c) size distribution curve of the two groups of fibers showing significant differences in their diameters ($p < 0.05$). $n = 100$ for each sample.

C—O—C stretching), and 1157 cm^{-1} (C—O stretching in amorphous phase). In the PCL Blank, a weak peak around 960 cm^{-1} (C—C stretching vibration) indicates the presence of the crystalline phase regions within polymeric structure. When P4 was added to the polymer solution, to become PCL dry, there were visual characteristic changes. There were additional peaks at 1661 cm^{-1} (C═C stretching), 1698 cm^{-1} (C═O stretching), and 2800–3000 cm^{-1} (C—H stretching vibration) confirming P4 in the fiber as the pure P4 spectrum shows characteristic peaks at these wavelengths—this can be seen in PCL dry and PCL wet. The diminishing peaks between 1160 and 1190 cm^{-1} from the PCL and between 500 and 1000 cm^{-1} from the P4, seen in the PCL dry fibers signify reduction in the crystallinity and thereby indicating some degree of solid dispersion and the formation of an amorphous mixture of the polymer and drug. In fibers, there were small peaks around 3440 and 670 cm^{-1} which can be attributed to water vapor and CO_2, respectively, in the air.[58,59] Once PS80 was added to the polymer solution to become PCL wet, there were peaks around 2870–2900 cm^{-1} (CH_2) representing asymmetric and symmetric bands, and also a stretching band at 1735 cm^{-1} (C═O ester group).[60] The diminishing bands in Figure 3C,D, at around 1600 and 1485 cm^{-1} suggest further reduction in crystallinity within the fiber which can be attributed to the improved solubility of the drug and therefore the drug release profile.[61]

3.4. Drug Diffusion

The calibration curves for this study are given in Figure S2 (Supporting Information). The drug loading in PCL dry and PCL wet fibers samples being tested (11.9 mg) is 4.4 mg ± 0.001 and 6.1 mg ± 0.001, respectively. Common transdermal patches weigh approximately between 500 and 2000 mg, and for current patches that include combined P4 and estrogen, the level of P4 ranges approximately between 6 and 11.2 mg, therefore confirming the relative higher drug loading in overall lower polymeric patch weight.[62,63] The total of 11.9 mg of PCL wet results in the delivery of 6.1 mg of P4 into PBS over a 20-h period, enabling a personalized approach of P4 delivery with the tailored weight of the PCL wet patch according to each patient's needs. For instance, a 40 mg patch of PCL wet can potentially achieve the guideline-recommended approach of approx. 20 mg of P4

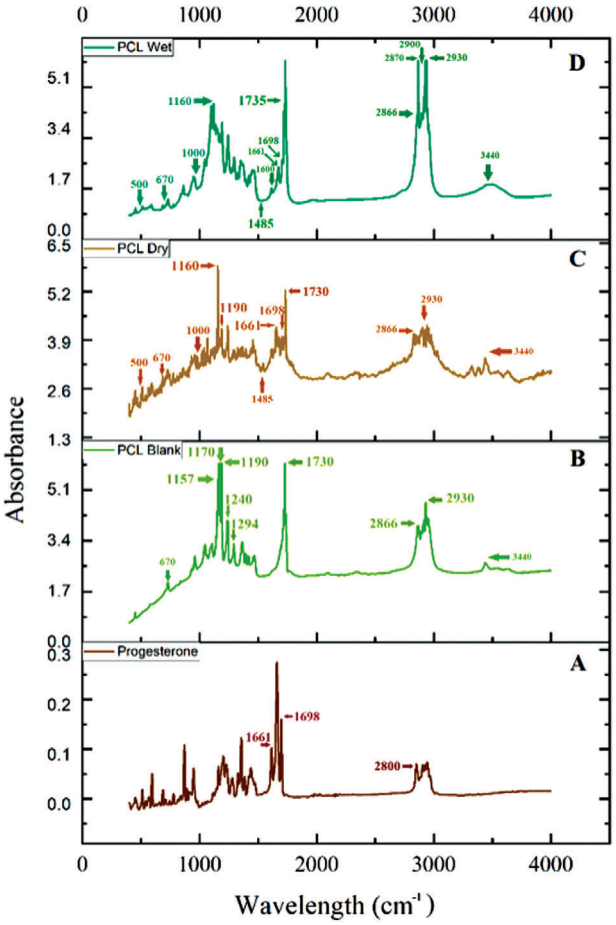

Figure 3. Analysis on A) P4, B) PCL blank, C) PCL dry, and D) PCL wet.

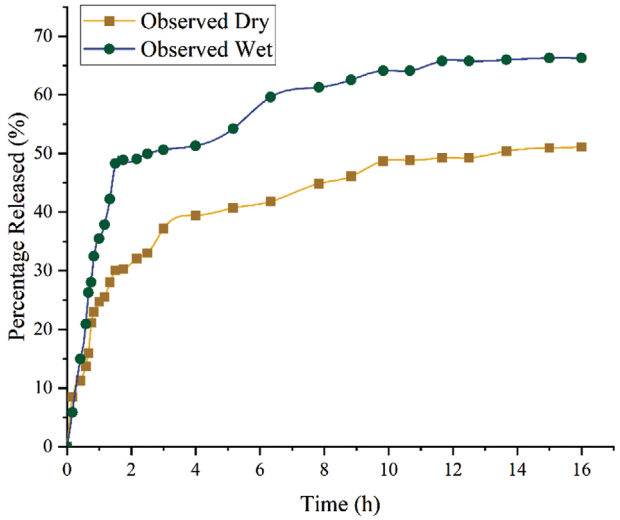

Figure 4. Observed Transdermal P4 Release into PBS ($p < 0.05$).

delivery.[15] Preclinical toxicity studies reveal progesterone's LD50 (lethal dose, 50%) values—100 mg kg^{-1} in mice, 327 mg kg^{-1} in rats, and 26.5 mg kg^{-1} in rabbits—far exceeding the therapeutic doses for current endometrial therapy, underscoring its safety.[64]

Observed dry and observed wet is the experimental drug release data from PCL dry and PCL wet drug release studies. There was a statistically significant difference in drug release when incorporating polysorbate into the fibers ($p < 0.05$). The incorporation of PS80 into the fiber patches increased drug loading and drug release, as seen in **Figure 4**. During the study, the PCL dry fibers achieved 51% drug release, while the wet fibers reached 66% drug release. The graph suggests an initial burst release within the first 3 h, with the dry fibers releasing ≈30% and the wet fibers releasing around 50% of progesterone (PCL dry and PCL wet, respectively). The initial burst release observed can be ascribed to the high concentration of P4 released from the porous surface property of PCL. The presence of highly volatile acetone might have contributed to the porosity of the patch, facilitating the easier release of the drug.[65,66] After the initial burst, there is a gradual and sustained release of P4 from the fibers. Around the 17-h mark, there is a spike in P4 release. This is due to the erosion of the PCL polymer allowing for a considerable increase in P4 release toward the end of the experiment, and therefore the drug release halted at this point.[67] The rapid drug release from the wet fibers is accredited to the surfactant characteristic, which increases the hydrophilicity of the dosage.[25] Additionally, the FTIR analysis revealed that the P4 fiber may become more amorphous due to this property, leading to further drug dissolution. The surfactant's interaction with lipid bilayers in the skin, enhancing drug permeability, is paralleled in its effect on the cellulose acetate membrane. It disrupts and alters the organized array, creating a more relaxed layout and augmented membrane permeability. This results in an increase in the sub-structural porosity and consequently, increased drug permeation.[25,26,68] Such interactions offer insights into how polysorbate 80 might operate in ex vivo scenarios, and by extension, in in vivo conditions.

As the standard deviation is too small to be seen using error bars on the graph, the variability of the range of standard deviation values are as follows: for PCL dry, the standard deviation value range is (0.025–0.061), the average of this range is 0.05, and the variance of this range is 7.2E-05. For PCL wet, the standard deviation value range is (0.0015–0.026), the average of this range is 0.014, and the variance of this range is 5.6E-05. The range of standard deviation values is wider for PCL dry compared to PCL wet. This indicates that PCL dry exhibits greater variability or spread of data points in terms of drug release. The smaller variance value

Table 5. Average RMSE between observed and predicted models.

Models	Average RMSE
Makoid Banakar	3
Higuchi	9.5
Gompertz	2.6
Korsemeyer Peppas	4.4
Makoid Banakar	7.3
Peppas Sahlin	3
Probit	3.2
Weibull	2.5
Hopfenberg	15.3
Geometric Model	3.3

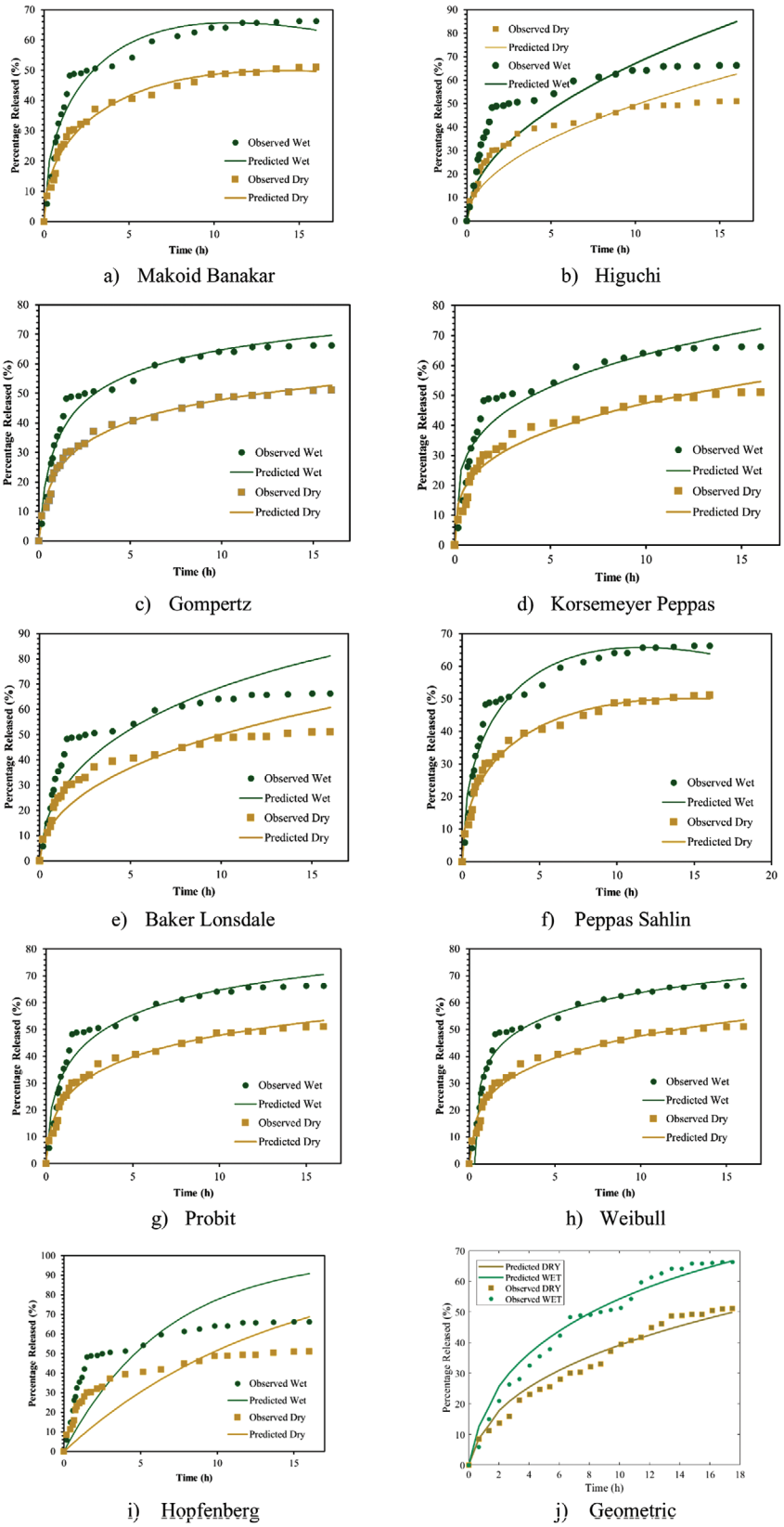

Figure 5. Fitting Of kinetic release models for transdermal P4 release into PBS. The experimental data were fit into the various release models (a-j) to determine which model best describes progesterone release from PCL fibres under the influence of polysorbate 80.

Table 6. Constants for the Models.

Models	Dry Parameters	Wet Parameters
Makoid Banakar	$k_{MB} = 22.475$, $n = 0.456$, $k = -0.032$	$k_{MB} = 34.645$, $n = 0.459$, $k = -0.042$
Higuchi	$k_H = 15.65$	$k_H = 21.232$
Gompertz	$\alpha = 1.082$, $\beta = 0.911$	$\alpha = 1.461$, $\beta = 0.684$
Korsemeyer Peppas	$k_{KP} = 23.507$, $n = 0.304$	$k_{KP} = 34.232$, $n = 0.269$
Baker Lonsdale	$k_{BL} = 0.006$	$k_{BL} = 0.012$
Peppas Sahlin	$k_1 = 26.306$, $k_2 = 3.454$, $m = 0.498$	$k_1 = 39.365$, $k_2 = -5.887$, $m = 0.493$
Probit	$\alpha = -0.733$, $\beta = 0.679$	$\alpha = -0.420$, $\beta = 0.797$
Weibull	$\alpha = 3.495$, $\beta = 0.356$, $T_i = 0.145$	$\alpha = 1.915$, $\beta = 0.293$, $T_i = 0.403$
Hopfenberg	$k_{HB} = 6.06 \times 10^{-5}$, $n = 1196.848$	$k_{HB} = 2.37 \times 10^{-5}$, $n = 6299.214$
Geometric Model	$\gamma = 2.415$, $D_{dry} = 6\ cm^2\ s^{-1}$	$\gamma = 2.415$, $D_{wet} = 124\ cm^2\ s^{-1}$

for PCL wet indicates that the standard deviation values within this dataset are more consistent or less variable compared to PCL dry, suggesting a tighter cluster of data. Encapsulation efficiency is 42% and 76% for PCL dry and PCL wet patches, suggesting that PS80 contributed to the increase in drug loading into the fibers.

3.5. Predictive Models

The mathematical models are overlaid upon the observed drug release data in Figures. The Hopfenberg Model (**Figure 5i**) had the greatest average RMSE across both wet and dry fibers, with an RMSE of 15.3, while the Weibull model (Figure 5h) had the smallest average RMSE, with an RMSE of 2.5. **Table 5** presents all of the RMSE results. As anticipated and shown in **Table 6**, the empirical release constants were notably higher when the P4 loaded fibers were infused with polysorbate, owing to the faster overall wet fiber release compared to dry fiber release. The Weibull model has the lowest average RMSE, indicating that this model provided the closest fit to the experimental data. The other models had higher RMSE values, suggesting a less accurate model of the drug release behavior. This highlights the model's versatility and potential for modeling hydrophobic drug release from fibers.

4. Conclusions

The objective was to develop a transdermal fibrous patch that could deliver high doses of P4 for potential applications in endometrial cancer treatment. With the high solubility of P4 in acetone, a high P4 dose was incorporated into the fibrous patch. The patch was characterized to determine its properties, with a focus on the impact of PS80 on the polymer solution rheology, fiber diameter, composition, morphology, and drug release. The addition of PS80 to the polymer solution reduced viscosity and surface tension, increased fiber diameter, and improved P4 permeation through the cellulose acetate membrane. However, excess PS80 resulted in unsuccessful fiber generation. FTIR analysis indicated that both P4 and PS80 had an impact on the absorbance curves, and the surfactant increased the hydrophilicity of the poorly soluble P4, which may have contributed to the formation of an amorphous solid mixture of PCL and P4 in the fiber. This enhanced the release and transport of P4 across the cellulosic membrane, suggesting that the use of an ideal surfactant could improve the transmucosal potential of drug-loaded P4 fibers. Mathematical modeling revealed that the Weibull model provided the best fit. By using acetone, high amounts of P4 were successfully loaded into the fiber patches and released in an in vitro system, demonstrating their potential for transdermal high-dose P4 drug delivery in gynecological oncology. In summary, this study centers on the development of a transdermal fibrous patch for high-dose P4 delivery. While primarily exploring drug release from fibers, it highlights the potential of using fine fibers to deliver P4 via the transdermal route. To realize the clinical potential of this approach, further studies are needed to evaluate its efficacy and safety in vivo. Future investigations should also focus on creating an adhesive backing layer to ensure proper adherence to the skin, advancing this innovative drug delivery approach closer to practical application.

The study successfully demonstrated P4 permeation through a cellulose acetate membrane in PBS system, highlighting the role of PS80. Some inherent limitations exist with the test, such as the difference between cellulose acetate membrane and real skin. Further studies using porcine skin are logical areas of follow-up research. Additionally, an MTT Assay will ascertain the biocompatibility of the polymeric fibers. Building on the outcomes of this study will enhance our understanding of fibrous drug release and its clinical significance.

Supporting Information

Supporting Information is available from the Wiley Online Library or from the author.

Acknowledgements

O.S. would like to thank the Sir Richard Stapley Educational Trust for the financial support throughout his Ph.D. studies. Also, O.S. wishes to thank London Gynaecology for access to the clinical environment and expertise to supplement the research experience.

Conflict of Interest

The research was conducted in the absence of any commercial or financial relationships.

Author Contributions

O.S., Ph.D. Student, created the research followed by visualization, characterization, analysis, and wrote the original draft. S.P., Consultant Gynecological Oncologist oversaw the clinical literature. U.H.C., Undergraduate Mechanical Engineering Student, supported O.S. with experimental studies. F.B., Senior lecturer of Pharmacy, optimized analysis and contributed to the pharmaceutical contributions and manuscript editing. M.E., FRENG, OBE, optimized paper writing and provided overall supervision of the manuscript and research project. All authors contributed to the research and approved the final version.

Data Availability Statement

The data that support the findings of this study are available in the supplementary material of this article.

Keywords

drug release, electrospinning, functional biomaterials, gynecology, oncology, palliative care, polycaprolactone, polysorbate, progesterone

Received: December 14, 2023
Revised: February 15, 2024
Published online:

[1] J. F. R. Sankaranarayanan, *Best Pract. Res. Clin. Obstet. Gynaecol.* **2006**, *20*, 207.
[2] P. Williams, M.-C. Rebeiz, L. Hojeij, S. J. McCall, *Br. J. Gen. Pract.* **2022**, *72*, e849.
[3] K. Njoku, C. E. Barr, E. J. Crosbie, *Front Oncol.* **2022**, *12*, 890908.
[4] Cancer Research UK, Uterine cancer statistics | Cancer Research UK, https://www.cancerresearchuk.org/health-professional/cancer-statistics/statistics-by-cancer-type/uterine-cancer#heading-Zero (accessed: November 2021).
[5] J. B. Pakish, K. H. Lu, C. C. Sun, J. K. Burzawa, A. Greisinger, F. A. Smith, B. Fellman, D. L. Urbauer, P. T. Soliman, *J. Women's Health* **2016**, *25*, 1187.
[6] V. Kurra, K. M. Krajewski, J. Jagannathan, A. Giardino, S. Berlin, N. Ramaiya, *Cancer Imaging* **2013**, *13*, 113.
[7] T. Luu, *Front Oncol.* **2022**, *12*, 1.
[8] T. Watt, R. Sullivan, A. Aggarwal, BMJ Open **2022**, *24*, 12.
[9] G. Giannone, D. Castaldo, V. Tuninetti, G. Scotto, M. Turinetto, A. A. Valsecchi, M. Bartoletti, S. Mammoliti, G. Artioli, G. Mangili, V. Salutari, D. Lorusso, G. Cormio, C. Zamagni, A. Savarese, D. Maio, G. Ronzino, C. Pisano, S. Pignata, G. Valabrega, *Front Oncol.* **2022**, *12*, 1.
[10] J. Weishaupt, K. Sivasubramaniyam, *Aust. N. Z. J. Obstet. Gynaecol.* **2019**, *59*, 20.
[11] S. Yang, K. W. Thiel, K. K. Leslie, *Trends Endocrinol. Metab.* **2011**, *22*, 145.
[12] NHS, H., (HRT) –NHS, https://www.nhs.uk/conditions/hormone-replacement-therapy-hrt/ (accessed: November 2021).
[13] J. J. Kim, E. Chapman-Davis, *Semin. Reprod Med.* **2010**, *28*, 081.
[14] N. Colombo, C. Creutzberg, F. Amant, T. Bosse, A. González-Martín, J. Ledermann, C. Marth, R. Nout, D. Querleu, M. R. Mirza, C. Sessa, *Int. J. Gynecol. Cancer.* **2016**, *26*, 2.
[15] RCOG Green-top Guideline No. *RCOG/BSGE Jt. Guidel.* **2016**. https://www.rcog.org.uk/guidance/browse-all-guidance/green-top-guidelines/management-of-endometrial-hyperplasia-green-top-guideline-no-67/Ac (accessed: December 2022)
[16] J. Varughese, S. Richman, *Rev. Obstet. Gynecol.* **2010**, *3*, 122.
[17] R. J. Paulson, M. G. Collins, V. I. Yankov, *J. Clin. Endocrinol. Metab.* **2014**, *99*, 4241.
[18] J. M. Brown, E. Poirot, K. L. Hess, S. Brown, M. Vertucci, M. Hezareh, *PLoS One* **2016**, *11*, e0151378.
[19] R. Galzote, S. Rafie, R. Teal, S. Mody, *Int. J. Womens Health* **2017**, *9*, 315.
[20] D. Crook, in *Managing the Menopause*, Cambridge University Press, Cambridge **2015**, pp. 118–123.
[21] X. Duan, H. Chen, C. Guo, *J. Mater. Sci. Mater. Med.* **2022**, *33*, 78.
[22] N. Talebi, D. Lopes, J. Lopes, A. Macário-Soares, A. K Dan, R. Ghanbari, K. H. Kahkesh, D. Peixoto, P. S. Giram, F. Raza, F. Veiga, E. Sharifi, H. Hamishehkar, A. C. Paiva-Santos, *Appl. Mater. Today* **2023**, *30*, 101726.
[23] G. Cevc, *Expert Opin. Investig. Drugs* **1997**, *6*, 1887.
[24] M. R. Prausnitz, V. G. Bose, R. Langer, J. C. Weaver, *Proc. Natl. Acad. Sci. U. S. A.* **1993**, *90*, 10504.
[25] M. Yasir, I. Som, K. Bhatia, *J. Pharm Bioallied Sci.* **2012**, *4*, 2.
[26] F. Han, S. Li, R. Yin, H. Liu, L. Xu, *Colloids Surf., A* **2008**, *315*, 210.
[27] E. J. Torres-Martinez, J. M. C. Bravo, A. S. Medina, G. L. P. González, L. J. V. Gómez, *Curr. Drug. Deliv.* **2018**, *15*, 1360.
[28] N.-I. Farkas, L. Marincaș, L. Barbu-Tudoran, R. Barabás, G. L. Turdean, *J. Funct. Biomater.* **2023**, *14*, 331.
[29] O. Shafi, M. Edirisinghe, F. Brako, *J. Drug Delivery Sci. Technol.* **2022**, *79*, 104062.
[30] C. Karuppannan, M. Sivaraj, J. G. Kumar, R. Seerangan, S. Balasubramanian, D. R. Gopal, *Nanoscale Res. Lett.* **2017**, *12*, 4.
[31] N. Alhusein, I. S. Blagbrough, P. A. de Bank, *Drug. Deliv. Transl. Res.* **2013**, *3*, 542.
[32] H. Majd, A. Harker, M. Edirisinghe, M. Parhizkar, *J. Drug Delivery Sci. Technol.* **2022**, *72*, 103359.
[33] N. Alhusein, I. S. Blagbrough, P. A. de Bank, *Drug. Deliv. Transl. Res.* **2012**, *2*, 477.
[34] R. Dwivedi, S. Kumar, R. Pandey, A. Mahajan, D. Nandana, D.S Katti, D. Mehrotra, *J. Oral Biol. Craniofacial Res.* **2020**, *10*, 381.
[35] D. Massella, F. Leone, R. Peila, A. A. Barresi, A. Ferri, *J. Funct. Biomater.* **2018**, *9*, 1.
[36] S. G. Er, T. A. Tabish, M. Edirisinghe, R. K. Matharu, *Front Med.* **2022**, *9*, 1.
[37] L. A. Bosworth, S. Downes, *J. Polym. Environ.* **2012**, *20*, 879.
[38] N. Akhtar, M. Rehman, H. Khan, F. Rasool, T. Saeed, G. Murtaz, *Trop. J. Pharm. Res.* **2011**, *10*, https://doi.org/10.4314/tjpr.v10i3.1.
[39] E. W. Group, EWG's Skin Deep, https://www.ewg.org/skindeep/browse/ingredients/705142POLYSORBATE80/?category=moisturizer (accessed: July 2023).
[40] A. Haq, *Drug Delivery* **2018**, *25*, 1943.
[41] I. Effendy, H. I. Maibach, *Contact Dermatitis* **1995**, *33*, 217.
[42] A. Haq, M. Dorrani, B. Goodyear, V. Joshi, B. Michniak-Kohn, *Int. J. Pharm.* **2018**, *539*, 58.
[43] R. Rajan, D. T. Vasudevan, *J. Adv. Pharm. Technol. Res.* **2012**, *3*, 112.
[44] A. Idrees, N. U. Rahman, Z. Javaid, M. Kashif, I. Aslam, K. Abbas, T. Hussain, *Acta Pol. Pharm.* **2014**, *71*, 287.
[45] P. S. Jain, A. J. Chaudhari, S. A. Patel, Z. N. Patel, D. T. Patel, *Pharm. Methods* **2011**, *2*, 198.
[46] D. Semnani, M. Afrashi, F. Alihosseini, P. Dehghan, M. Maherolnaghsh, *J. Mater. Sci. Mater. Med.* **2017**, *28*, 175.
[47] Y. Zhang, P. Qi, *Pharm. Sci. Biomed. Anal. J.* **2017**, *1*, 111.
[48] W. P. Wuelfing, K. Kosuda, A. C. Templeton, A. Harman, M. D. Mowery, R. A. Reed, *J. Pharm. Biomed. Anal.* **2006**, *41*, 774.
[49] Y. Zhang, M. Huo, M. J. Zhou, A. Zou, W. Li, C. Yaoand, S. Xie, *AAPS J.* **2010**, *12*, 263.
[50] M. Eltayeb, E. Stride, M. Edirisinghe, A. Harker, *Mater. Sci. Eng., C* **2016**, *66*, 138.
[51] K. Łupina, D. Kowalczyk, W. Kazimierczak, *Polymers* **2021**, *13*, 1062.

[52] M. H. Shoaib, S. A. S. Siddiqi, R. I. Yousuf, K. Zaheer, M. Hanif, S. Rehana, S. Jabeen, *AAPS PharmSciTech* **2010**, *11*, 708.
[53] I. Permanadewi, A. C. Kumoro, D. H. Wardhani, N. Aryanti, *J. Phys. Conf. Ser.* **2019**, *1295*, 012063.
[54] J. Yang, R. Pal, *Polymers* **2020**, *12*, 2302.
[55] A. R. D'Amato, M. T. K. Bramson, D. T. Corr, D. L. Puhl, R. J. Gilbert, J. Johnson, *Electrospinning* **2018**, *2*, 15.
[56] C. J. Angammana, S. H. Jayaram, *IEEE Trans. Ind. Appl.* **2011**, *47*, 1109.
[57] S. Ali, Z. Khatri, K. W. Oh, I. Kim, S. H. Kim, *Macromol. Res.* **2014**, *22*, 562.
[58] National Institute of Standards and Technology, https://webbook.nist.gov/cgi/cbook.cgi?ID=C124389&Type=IR-SPEC&Index=1 (accessed: January 2024).
[59] National Institute of Standards and Technology. https://webbook.nist.gov/cgi/cbook.cgi?ID=C7732185&Type=IR-SPEC&Index=1#IR-SPEC (accessed: January 2024).
[60] K. Pramod, C. V. Suneesh, S. Shanavas, S. H. Ansari, J. Ali, *J. Anal. Sci. Technol.* **2015**, *6*, 34.
[61] D. Ciolacu, F. Ciolacu, V. Popa, *Cellul. Chem. Technol.* **2011**, *45*, 13.
[62] EMC, Evorel Sequi, https://www.medicines.org.uk/emc/product/10930/pil. (accessed: July 2023)
[63] EMC, EVRA 203 micrograms/24 hours + 33.9 micrograms/24 hours transdermal patch, https://www.medicines.org.uk/emc/product/13054/smpc. (accessed: July 2023)
[64] R. Sitruk-Ware, *Climacteric* **2018**, *21*, 315.
[65] A. Ujčić, M. Sobótka, M. Šlouf, A. Różański, K. Szustakiewicz, *Polym. Test.* **2022**, *118*, 107906.
[66] E. Altun, J. Ahmed, M. O. Aydogdu, A. Harker, M. Edirisinghe, *Eur. Polym. J.* **2022**, *173*, 111300.
[67] H. R. Munj, J. J. Lannutti, D. L. Tomasko, *J. Biomater. Appl.* **2017**, *31*, 933.
[68] S. Bolandi, F. Z. Ashtiani, A. Okhovat, M. B. Ghandashtani, *Theor. Found. Chem. Eng.* **2020**, *54*, 931.

